Monte Carlo Simulation of Polyelectrolyte Gels: Effects of Polydispersity and Topological Defects

Samuel Edgecombe* and Per Linse

Physical Chemistry 1, Center for Chemistry and Chemical Engineering, Lund University, P.O. Box 124, S-221 00 Lund, Sweden

Received January 9, 2007; Revised Manuscript Received March 20, 2007

ABSTRACT: Volumes and other structural properties of polyelectrolyte gels in equilibrium with pure water have been determined by Monte Carlo simulations. The role of chain length polydispersity and topological network defects of four different networks with varying cross-linking density, monomer charge, and chain stiffness have been investigated. Generally, a chain length polydispersity reduced the gel volume, whereas the presence of chains with one end detached from the cross-linker (severed chains) led to an increased gel volume. Polyelectrolyte networks displayed the largest and uncharged polymer networks the smallest dependence on chain length polydispersity. The effect of severed chains was strongest for flexible polyelectrolyte gels and weakest for uncharged networks and stiff polyelectrolyte gels. Mechanical properties of uncharged and charged polymer gels were also investigated through uniaxially stretching and compared with theory.

1. Introduction

Polyelectrolyte gels are networks of cross-linked polyelectrolytes. Such gels possess unique swelling and elastic properties of strong scientific interest and of vital technological use. Swollen polyelectrolyte gels, often referred to as hydrogels, are used in, e.g., drug delivery formulations,[1] eye lenses, superabsorbants, and agriculture as humidity controllers.[2]

There are two main routes to synthesize networks: (1) cross-linking polymers (macromonomers) possessing reactive end groups with cross-linkers and (2) cross-linking a mixture of monomers and cross-linkers. Both methods result in networks with topological defects such as pendant chains, loops, and entanglements. Whereas networks made from method (1) have a controlled chain length distribution, viz. the distribution of the macromonomers, method (2) produces networks with an unknown chain length distribution. The characterization of the length polydispersity of network chains is technically difficult, and hence the effect of the polydispersity on the gel properties is hard to assess.

Simulation techniques, such as Monte Carlo simulations and molecular dynamics, are two indispensable methods to examine fundamental properties of systems at well-defined compositions and/or at conditions not easily experimentally accessible. Escobedo and de Pablo[3] have recently revised the use of these methods to examine uncharged polymer gels, and Everaers[4] has given an extensive review of different theories and provided simulation results illuminating the role of entanglements in polymer networks. Furthermore, simulation methods have also been used to investigate polyelectrolyte gels,[5−13] including the occurrence of first-order transition,[7,9] effect of added salt,[10] and oppositely charged macromolecules.[13]

Experimentally, uncharged polymer gels made from a bimodal chain length distribution have been known to give a mechanically stronger gel originating from the finite extensibility of chains.[14−19] Kilian[20] was able to reproduce the stress−strain curves obtained by Zhang and Mark[18] for bimodal poly(dimethylsiloxane) (PDMS) networks using a van der Waals equation of state and considering that short chains behaved as rigid rods in the limit of small elongations. Erman and Mark calculated the mechanical properties of networks with a trimodal chain length distribution and concluded that these networks should be stronger than bimodal ones.[21] Simulations of networks possessing a bimodal chain length distribution have been performed but limited to neutral networks.[22−26] Experimental studies of the swelling of uncharged polymer networks from mono- and bifunctional end-linked polymers showed a slight increase in the swelling as the fraction of monofunctional chains increased.[27,28]

The present study is focused on how properties of polyelectrolyte gels in equilibrium with pure water are affected by (i) chain length polydispersity and (ii) topological network defects arising from incomplete cross-linking leading to pendant chains. Gel volume and other structural properties of a coarse-grained model of polyelectrolyte gels with polydisperse chain lengths or pendant chains have been determined from Monte Carlo simulations. In particular, we found that chain length polydispersity generally decreases the gel volume, whereas an incomplete cross-linking leads to an increased gel volume. The magnitude of these effects was strongly dependent on other properties of the polyelectrolyte gel.

2. Model

2.1. General Properties. A coarse-grained approach based on the primitive model of electrolytes has been used to describe polyelectrolyte gels. We have adopted basically the same model as in previous studies of polyelectrolyte gels from our laboratory.[5,6,9,10]

The systems of interest are composed of a positively charged network with negatively charged counterions dissolved in excess of water. All charged particles are treated explicitly as charged hard spheres, whereas the solvent is modeled as a dielectric continuum. The network is composed of chains that are end-connected to tetrafunctional cross-linkers (nodes). The network topology is conserved during the simulation. The chains consist of hard spheres (beads) that are connected by harmonic springs. Beads and nodes will collectively be referred to as network particles. These particles carry the same charge $z_{bead} = z_{node}$ and possess the same radius $R_{bead} = R_{node} = 2$ Å. The average

10.1021/ma0700633 CCC: $37.00
Published on Web 04/21/2007

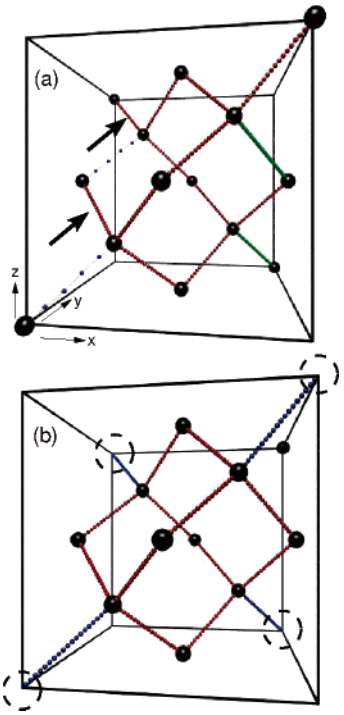

Figure 1. Snapshot of networks (in highly nonequilbrium states) of the reference system (one unit cell) with (a) polydisperse chain length distribution at $\gamma = 1.16$ and (b) severed chains at $p = 0.25$. Nodes (black spheres) have been made artifically larger for clarity. Color code: In (a), short chains (blue), medium-length chains (red), and long chains (green), and, in (b), active chains (red) and severed chains (blue). In (a), arrows indicate super-strained medium-length chains, and in (b), dashed circles indicate the free ends of the severed chains.

Table 1. General Data of the Model

node radius	R_{node}	2 Å
node charge	z_{node}	0 and +1
bead radius	R_{bead}	2 Å
bead charge	z_{bead}	0 and +1
small ion radius	R_{ion}	2 Å
small ion charge	z_{ion}	−1
av no. of beads per chain	$\bar{n}_{bead}$	20 and 40
temperature	T	298 K
relative permittivity	ϵ_r	80

number of beads per chain is denoted by $\bar{n}_{bead}$. The flexibility of the chains is regulated by a harmonic angular potential. There are n_{ion} simple monovalent ions with radius $R_{ion} = 2$ Å, compensating the net charge of the network. General data of the model are collected in Table 1.

A network with (i) chains of equal length and (ii) a defect-free diamond-like topology will be referred to as a *perfect* network. Such a network contains 8 nodes and 16 elastically active chains per unit cell. Two deviations from a perfect network will be investigated, viz networks with (i) a chain length polydispersity or (ii) topological defects.

2.1.1. Chain Length Polydispersity. A network with a polydisperse chain length distribution is composed of chains of different lengths. In particular, we will consider networks containing chains of three different lengths, sometimes referred to as trimodal networks.[21]

Unless otherwise stated, one unit cell contains $N_{chain,s} = 2$ short chains of length $n_{bead,s}$, $N_{chain,m} = 12$ medium-length chains of length $n_{bead,m} = \bar{n}_{bead}$, and $N_{chain,l} = 2$ long chains of length $n_{bead,l}$. The lengths of the short and long chains are varied with the constraint $n_{bead,s} + n_{bead,l} = 2\bar{n}_{bead}$, where $\bar{n}_{bead}$ is constant. Besides the monodisperse chain length distribution with $n_{bead,s} = n_{bead,l} = \bar{n}_{bead}$, we will examine several networks with a polydisperse chain length distribution. Polydisperse networks are characterized by their polydispersity index $\gamma = \bar{M}_m/\bar{M}_n$, where $\bar{M}_m$ denotes the mass average and $\bar{M}_n$ the number average.

Furthermore, if nothing else is stated, in a unit cell the two short chains connect the nodes located at *a* (0,0,0) and *a* (1/4, 1/4, 1/4) and the nodes located at *a* (0, 1/2, 1/2) and *a* (1/4, 3/4, 3/4), where *a* is the length of one unit cell. The two longest chains connect the nodes located at *a* (3/4, 3/4, 1/4) and *a* (1, 1, 0) and the nodes located at *a* (3/4, 1/4, 3/4) and *a* (1, 1/2, 1/2). Medium-length chains connect the remaining nearest-node pairs. Figure 1a illustrates this distribution of chains of different length in the network, which in short will be referred to as setup 1.

2.1.2. Topological Network Defects. Starting from the perfect network, topological network defects can be systematically introduced. Here, we remove bonds between chains and nodes to obtain chains which are attached to the network by only one of its two ends (referred to as severed chains). Such systems could be made experimentally *either* by using a mixture of mono- and bifunctional end-linking polymers[28] *or* by breaking node−bead bonds after cross-linking by using, e.g., a biologically or chemically degradable cross-linker like sucrose diacrylate.[29] Here, we remove node−bead bonds in a controlled manner such that the infinite connectivity of the network remains in all three dimensions. The parameter p denotes the fraction of chains being elastically inactive, i.e., chains having one free end. Hence, $p = 0$ implies no topological defects, and $p > 0$ represents networks with severed chains. Figure 1b illustrates the location of the inactive chains (blue) and their free ends (open circles) at $p = 0.25$.

2.2. Potential Energy. The potential energy U of a system can be expressed as a sum of four terms according to

$$U = U_{hs} + U_{elec} + U_{bond} + U_{angle} \tag{1}$$

The hard-sphere term U_{hs} is given by

$$U_{hs} = \sum_{i<j} u_{ij}^{hs}(r_{ij}) \tag{2}$$

where

$$u_{ij}^{hs}(r_{ij}) = \begin{cases} \infty & \text{if } r_{ij} < (R_i + R_j) \\ 0 & \text{if } r_{ij} \geq (R_i + R_j) \end{cases}$$

with R_i denoting the radius of particle i (node, bead, or small ion) and $r_{ij} = |\mathbf{r}_i - \mathbf{r}_j|$ the center-to-center distance between two particles. The electrostatic potential U_{elec} is given according to

$$U_{elec} = \sum_{i<j} \frac{z_i z_j e^2}{4\pi\epsilon_0\epsilon_r r_{ij}} \tag{3}$$

where z_i is the valence of particle i, e the elementary charge, ϵ_0 the permittivity of vacuum, and ϵ_r the relative permittivity of the solvent. The bond potential energy U_{bond} is given by

$$U_{bond} = \sum_{m=1}^{N_{bond}} \frac{k_{bond}}{2}(r_{m,bond} - r_0)^2 \tag{4}$$

where N_{bond} is the number of bonds in the network (node−bead and bead−bead bonds), $r_{m,bond}$ the length of bond m, $r_0 = 5$ Å the unperturbed equilibrium distance, and $k_{bond} = 0.4$ N/m the bond force constant. When all interactions are considered,

Table 2. Specification of Investigated Gel Systems and Their Equilibrium Volume for Perfect Networks

system	$z_{node} = z_{bead}$	$\bar{n}_{bead}$	k_{bond} (J/deg^2)	l_p^0 [a] (Å)	n_{ion} [b]	$\langle R_{bb}^2\rangle^{1/2}$ (Å)	$V_{perfect}$ [b] (10^6 Å^3)
ref	+1	20	0	7.0	328	6.10	8.85(3)
sys1	0	20	0	7.0	0	5.65	0.45(1)
sys2	+1	40	0	7.0	648	6.15	70.5(2)
sys3	+1	20	8.3×10^{-23}	370	328	6.05	20.6(1)

[a] The bare persistence length l_p^0 (the persistence length for a single, isolated, and uncharged chain) was evaluated according to $l_p^0 = \langle R_{bb}^2\rangle^{1/2}/(1 - \langle\cos\alpha\rangle)$.[37] [b] Per unit cell.

the root-mean-square (rms) bead-to-bead separation becomes $\langle R_{bb}^2\rangle^{1/2} \approx 6.0$ Å. Finally, the angular potential energy U_{angle} is given by

$$U_{angle} = \sum_{m=1}^{N_{angle}} \frac{k_{angle}}{2}(\alpha_m - \alpha_0)^2 \quad (5)$$

where N_{angle} is the number of polymer angles, α_m the angle of bond angle m formed by three consecutive beads in a chain, k_{angle} the angular force constant, and $\alpha_0 = 180°$ the unperturbed equilibrium angle.

2.3. Systems. Four different systems will be considered. One of these will be referred to as the reference (ref) system, and it is characterized by (i) monovalent node and bead charges, $z_{node} = z_{bead} = +1$, (ii) an average chain length $\bar{n}_{bead} = 20$, and (iii) fully flexible chains, $k_{angle} = 0$. As compared to the reference system, the network of system 1 (sys1) has a no charge, $z_{node} = z_{bead} = 0$, and hence no counterions; the network of system 2 (sys2) has longer chains, $\bar{n}_{bead} = 40$; and the network of system 3 (sys3) possesses stiffer chains, $k_{angle} = 8.3 \times 10^{-23}$ J/deg^2, corresponding to a bare persistence length $l_p^0 = 370$ Å. The specification of the different systems is given in Table 2. Each of these four systems has been examined as a perfect network and as several nonperfect networks.

The volume of the gel at equilibrium with pure water, V, is a central property. The gel volumes of the modified networks will be presented by using the volume ratio $V/V_{perfect}$, where V is the gel volume of the nonperfect network and $V_{perfect}$ the gel volume of the corresponding perfect network. Table 2 also provides the values of $V_{perfect}$. As compared to the reference system, the volume of the uncharged gel is 20-fold reduced, the volume of the polyelectrolyte gel with longer chains is 8-fold increased, and the volume of polyelectrolyte gel with stiff chains is 2.5 times larger. The reasons for these volume variations have previously been discussed.[6]

3. Simulation Details

Monte Carlo simulations were performed using the NVT (constant number of particles, constant volume, constant temperature) ensemble employing the Metropolis algorithm.[30] The particles were enclosed in a cubic box of length L, and periodic boundary conditions were applied. The long-range nature of the Coulomb interaction was handled by using the Ewald summation with conducting boundary conditions. Gel volume and force analyses were determined by using systems comprising one unit cell with $N_{node} = 8$ nodes and $N_{chain} = 16$ chains, whereas the other properties at equilibrium were examined using systems involving eight unit cells. Single translational displacements ranging from 2.5 to 5.0 Å were used for network particles and 10 Å for counterion particles. Acceptance ratios were typically 20% and 70% for network and counterion particles, respectively. The equilibration runs involved at least 10^4 passes (trial moves per particle) and the production runs at least 10^5 passes. The uncertainty of ensemble averages was taken from 10 block averages. Using a block averaging technique with extrapolation to infinite block length,[31] the statistical efficiency was found to be about 200; i.e., each of the 10 blocks comprises ~50 independent configurations. All simulations were performed using the integrated molecular dynamics/Monte Carlo/Brownian dynamics package MOLSIM.[32]

The osmotic pressure of the gel was evaluated as the sum of the ideal term, a virial term, and a contact term.[10] The volume of the gel in equilibrium with pure water were obtained from the simulated pressure−volume isotherms at zero osmotic pressure. Osmotic pressures obtained for systems represented by one and eight unit cells were statistically indistinguishable. The variation of the volume was made isotropically, That is fine for the perfect networks, where the networks are isotropic in the Cartesian directions, but leads to a small pressure unbalance among the Cartesian directions for the nonperfect networks.

The extension of chains was examined by considering their (i) rms end-to-end separation $\langle R_{ee}^2\rangle^{1/2}$ and (ii) Flory scaling exponent ν. The former was calculated according to

$$\langle R_{ee}^2\rangle^{1/2} = \langle(\mathbf{r}_{n_{bead}} - \mathbf{r}_1)^2\rangle^{1/2} \quad (6)$$

where $\mathbf{r}_i$ denotes the location of bead i in a chain. The Flory scaling exponent was evaluated from

$$\langle R_{ee}^2\rangle^{1/2} = \langle R_{bb}^2\rangle^{1/2}(n_{bead} - 1)^{\nu} \quad (7)$$

Averages were made separately over chains of different lengths (polydisperse network) and over active and inactive chains (topologically defected network).

4. Results

4.1. Chain Length Polydispersity. In the following, we will first examine how two specific issues affect the properties of the reference system with a polydisperse chain length distribution. Thereafter, we will investigate how such a polydisperse chain length distribution affects properties of the different systems described in Table 2.

4.1.1. Reference System. The influence of the distribution of chains of different length in the network has been investigated by employing three different distributions. Besides setup 1 previously presented in the Model section, two other setups have been used. Setup 2 is identical to setup 1 except that the two long chains now connect the nodes located at a(1/4, 1/4, 1/4) and a(0, 1/2, 1/2) and the nodes located at a(1/4, 3/4, 3/4) and a(0, 1, 1). The two short chains retain their location in the network as in setup 1, and the medium-length chains connect the remaining nearest-node pairs. In setup 3, the two short chains connect the nodes located at a(0, 0, 0) and a(1/4, 1/4, 1/4) and the nodes located at a(3/4, 3/4, 1/4) and a(1, 1, 0). The two long chains connect the nodes located at a(1/4, 1/4, 1/4) and a(1/2, 0, 1/2) and the nodes located at a(1/4, 3/4, 3/4) and a(1/2, 1/2, 1). Again, medium-length chains connect the remaining nearest-node pairs.

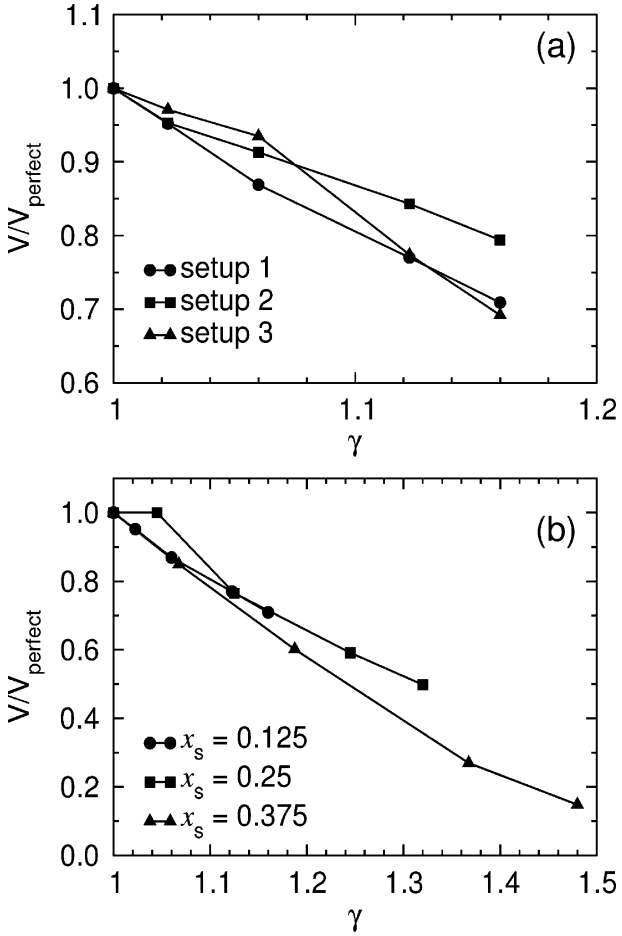

Figure 2. Volume ratio $V/V_{perfect}$ as a function of the polydispersity index γ for the reference system with (a) different distributions of chains of different length in the network according to setups 1−3 and (b) three different fractions of short chains $x_s = 0.125$, 0.25, and 0.375. Errors are smaller than the symbol size.

Figure 2a shows the equilibrium volumes for the three setups studied for the reference system at $\gamma = 1-1.16$, the latter corresponding to $n_{bead,s} = 4$ and $n_{bead,l} = 36$. First, the equilibrium volumes of the polyelectrolyte gel reduce as the polydispersity increases, and at $\gamma = 1.16$ the swelling is 20−30% lower than that for the perfect network. When $\gamma > 1.1$, the reduction of the swelling is found to depend on the distribution of chains of different length in the network. In more detail, the swelling curves for setups 1 and 3 superimpose. On closer comparison, we observe that for both setup 1 and 3 their shortest paths through the network are closely related. These consist of two short plus two medium-length chains, but in different order. In setup 2, which does not decrease in volume with increasing γ as much as the other two setups, the shortest path through the network consists of one short plus three medium length chains. Thus, we conjecture that a reduced length of the topological shortest path in the network causes the smaller equilibrium volume for gels at otherwise identical polydispersity index.

We will now examine how the equilibrium volume of the polyelectrolyte gel depends on the variation of the fraction of chains of the different lengths. The number of the short chains $N_{chain,s}$ and of the long chains $N_{chain,l}$ is kept equal, preserving $\bar{n}_{bead}$. The fraction of short chains is given by $x_s = N_{chain,s}/N_{chain}$, where N_{chain} is the total number of chains. We have selected to examine the cases $N_{chain,s} = 2$, 4, and 6 short chains per unit cell, corresponding to the fractions of short chains $x_s = 0.125$, 0.25, and 0.375, respectively.

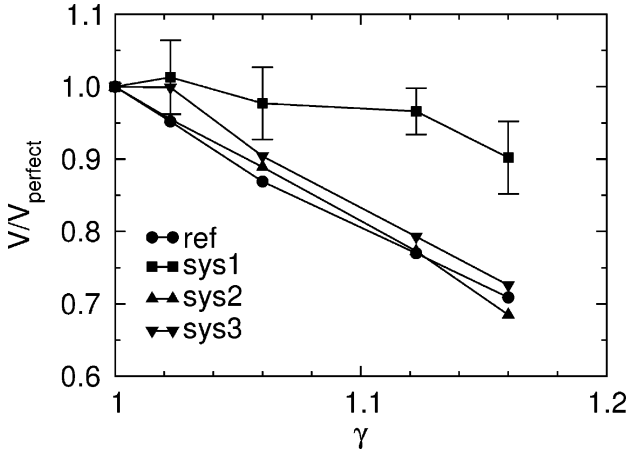

Figure 3. Volume ratio $V/V_{perfect}$ as a function of the polydispersity index γ for the reference system and systems 1−3. Errors are smaller than the symbol size except for system 1.

Figure 2b displays the equilibrium volumes as a function of γ for the different values of x_s. Note for increasing values of x_s, but under otherwise identical consitions, γ is increasing. When viewing the equilibrium volume as a function of γ, the swelling for the different fractions of chains of different lengths (i) is essentially independent of x_s at small γ and (ii) is weakly dependent on x_s at larger values of γ. Thus, the main effect of increasing the number of short and long chains while decreasing the number of medium-length chains is to reduce the equilibrium volume. Again, we attribute this volume reduction to the reduction of the topological shortest path in the network. Finally, we notice that at $\gamma = 1.5$ the equilibrium volume has reduced 7-fold as compared to the perfect network.

4.1.2. Comparison among the Different Systems. Various properties of the reference system and systems 1−3 will now be investigated. In the following, $N_{bead,s} = 2$, $N_{bead,m} = 12$, and $N_{bead,l} = 2$ will be used in conjunction with the distribution of the chains of different lengths in the network according to setup 1.

Figure 3 shows the volume ratio $V/V_{perfect}$ as a function of the polydispersity index γ for the different systems. Generally, the gel volume becomes smaller as the chain length polydispersity is increased. However, the polydispersity affects the gel volume differently among the four systems.

In more detail, the reference system displays a reduction of the volume ratio from $V/V_{perfect} = 1$ to 0.72 as γ is increased from 1 to 1.16. Hence, a polydispersity index of 1.16 reduces the gel volume by ≈25%. For the uncharged network (system 1), $V/V_{perfect}$ remains approximately unity at $\gamma = 1.06$ and decreases to 0.92 at $\gamma = 1.16$. Hence, the volume of uncharged polymer gels is weakly dependent on chain length polydispersity, which agrees with recent simulations of similar uncharged polymer networks.[23] The reduced swelling of the system with the longest average network chain length (system 2) displayed similar sensitivity on the polydispersity as the reference system. Thus, by increasing the average network chain length from 20 to 40, the effect of the polydispersity on the gel volume is essentially unaffected. System 3 has stiffer chains as compared to the reference system. Here we observed a slightly smaller reduction of the gel volume as the chain lengths are made polydisperse as compared to the reference system.

To further characterize the gels and better understand their equilibrium volumes, the extension of the chains in the networks have also been evaluated. Table 3 provides rms end-to-end separations and extension ratios of the chains of the different systems at selected values of γ investigated.

Table 3. Root-Mean-Square End-to-End Separation and Flory Scaling Exponent for Short, Medium-Length, and Long Chains in Polydisperse Networks [a]

system	γ	$\langle R_{ee,s}^2\rangle^{1/2}$ (Å)	$\langle R_{ee,m}^2\rangle^{1/2}$ (Å)	$\langle R_{ee,l}^2\rangle^{1/2}$ (Å)	ν_s	ν_m	ν_l
	1		81.2			0.88	
ref	1.06	45.3	81.0	103.7	0.91	0.88	0.84
	1.16	17.5	81.1	107.1	0.96	0.88	0.79
	1		35.4			0.62	
sys1	1.06	23.9	36.0	44.1	0.67	0.63	0.62
	1.16	24.1	34.8	41.1	0.67	0.63	0.60
	1		168.7			0.90	
sys2	1.06	96.0	169.0	221.0	0.92	0.90	0.88
	1.16	40.0	168.0	214.0	0.92	0.90	0.84
	1		110.2			0.99	
sys3	1.06	52.8	105.4	149.2	1.00	0.99	0.98
	1.16	20.4	110.2	166.2	0.99	0.98	0.96

[a] $N_{chain,s} = 2$, $N_{chain,m} = 12$, and $N_{chain,l} = 2$ with setup 1 were used throughout. Maximum uncertainties: $\sigma(\langle R_{ee}^2\rangle^{1/2}) = 0.9$ Å. The Flory exponents were calculated according to eq 7.

First, independently of the system, $\langle R_{ee,s}^2\rangle^{1/2} < \langle R_{ee,m}^2\rangle^{1/2} < \langle R_{ee,l}^2\rangle^{1/2}$ was obtained. Thus, the longer chains occupy larger space as compared to the shorter ones. This might not be totally unexpected because the significant difference in the number of beads among the chains of different length.

We will now focus on the stretching of the chains as reported by their Flory scaling exponents in Table 3. For all systems, we observe (i) $\nu_s > \nu_m > \nu_l$ for polydisperse chain length distributions, and (ii) ν_m is basically independent of the polydispersity index γ, whereas ν_s increases and ν_l decreases at increasing γ. In other words, observation (i) implies that in these systems the short chains are those most stretched and the long chains those least stretched. This finding is consistent with experimental results by Mark et al.,[21] who studied uniaxial stretching of trimodal gels made from short, medium-length, and long PDMS chains and showed that the short chains reached their maximum extension at low uniaxial extensions, while medium-length and long chains became fully extended first at much higher extensions. Observation (ii) means that the stretching of the short chains increases, while that of the medium-length chains is essentially constant, and that of the long ones reduces at increasing polydispersity. As a consequence, chains with $\bar{n}_{bead} = 20$ beads are less stretched at $\gamma = 1$ in the reference system ($\nu_m = 0.88$) than as the shortest ones at $\gamma = 1.06$ in system 2 ($\nu_s = 0.92$). Figure 4a shows a snapshot of the reference system at $\gamma = 1.16$ and the unequal stretching of chains of different length is evident. Regarding the uncharged network (system 1), the values of ν are smaller. Since $\nu_m = 0.62$ is larger than that expected for chains in a good solvent, $\nu = 0.588$,[33] these medium-length chains still remain weakly stretched. The short chains are more stretched than the longer ones, just as for the reference system and system 2. Finally, for the polyelectrolyte gel with stiff chains (system 3), ν is close to unity and hence these chains behave nearly as rigid rods.

The average force in individual bonds of the chains in the network is also of great value for characterizing the state of swollen gels. The average bond force of bond m is given by $\langle F_{bond,m}\rangle = -k_{bond}\langle r_{bond,m} - r_0\rangle$ (see eq 4). Figure 5 shows the average bond force as a function of the bond rank, i_{bond}, of all the chains in a single unit cell for all systems in the case of the monodisperse ($\gamma = 1$) and a polydisperse ($\gamma = 1.16$) network.

First two general observations. The average bond forces are always negative. Hence, all bonds are extended as compared to their unperturbed equilibrium distance r_0; hence, we have a bond tension, which is consistent with the conformational stretching of the chains. Second, the magnitude of the average bond force is largest for the bonds connecting the nodes.

A comparison of the bond tension among the different systems with monodisperse networks (Figure 5, left column)

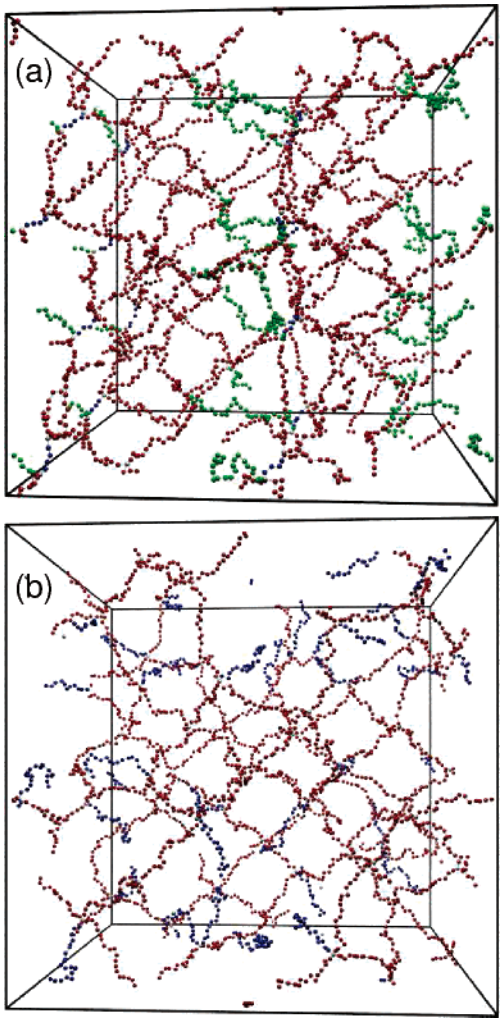

Figure 4. Snapshots of networks at equilibrium of the reference system (eight unit cells) with (a) polydisperse chain length distribution at $\gamma = 1.16$ and (b) severed chains at $p = 0.25$. Color code: In (a), short chains (blue), medium-length chains (red), and long chains (green), and in (b), active chains (red) and severed chains (blue). The box lengths are (a) $L = 370$ Å and (b) $L = 450$ Å.

shows some additional and interesting features. In charged networks (reference system and systems 2 and 3), as compared to uncharged ones (system 1), (i) the bond tension is ca. twice as large, (ii) the bond tension at the chain ends increases more, and (iii) the end effects affect a larger fraction of the chain. Issue (i) is of course related to the larger equilibrium volume (see Table 2), which originates from the fact that the osmotic pressure contribution from the counterions exceeds that arising

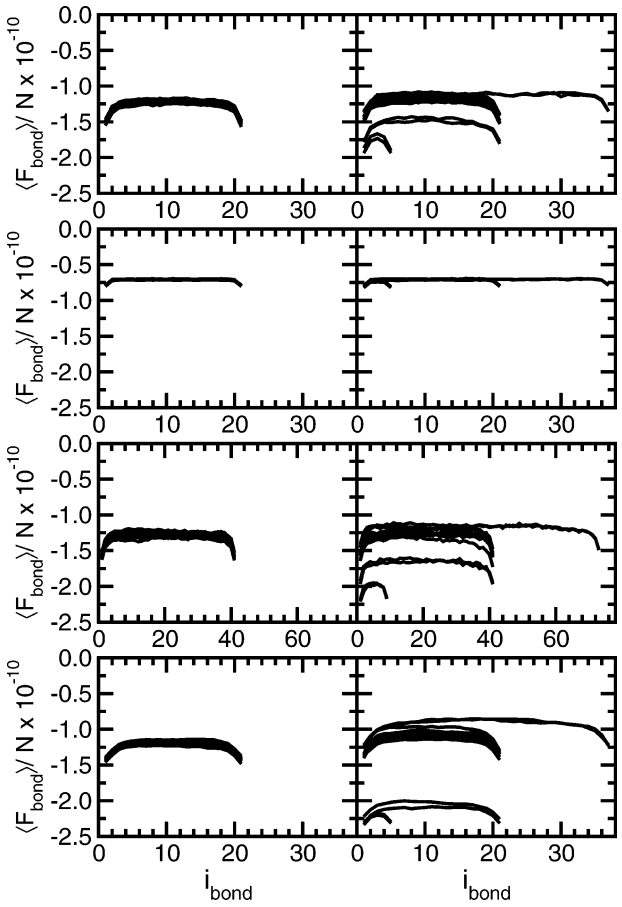

Figure 5. Average bond force (F_{bond}) as a function of the bond rank i_{bond} for all chains in one unit cell for (a) the reference system, (b) system 1, (c) system 2, and (d) system 3 at chain length polydispersity (i) $\gamma = 1$ and (ii) $\gamma = 1.16$. The first and last bonds are node−bead bonds.

from the excluded-volume interaction among the network particles. Issues (ii) and (iii) arise from a combination of the larger bead concentration appearing at the chain ends and the long-range nature of the repulsive Coulomb interaction, as compared to the short-range excluded-volume interaction. The larger range of the end effect in system 2 compared to the reference system is due to the longer screening length in system 2; i.e., in the reference system there is a higher accumulation of counterion charges around a node than in system 2.

When introducing chain length polydispersity, again the charged and uncharged gels displayed different behavior (Figure 5, right column). In the uncharged gels, the bond tension in the chains of different chain length were practically the same [panel (b.ii)]. Regarding the charged gels, the shortest chains displayed the largest bond tension, whereas the longest ones the smallest bond tension. Moreover, the set of average bond force curves for the medium-length chains separates into two groups. This heterogeneous separation appears due to different surroundings of the medium-length chains. The two arrows in Figure 1a point on the two medium-length chains with the largest bond tension. These chains are connected to two nodes which, in turn, are both bonded to a short chain. Other medium-length chains are connected to nodes of which at most one is bonded to a short chain. The heterogeneous separation is strongest for the network with the stiff chains, presumably since this network displays the largest gel volume.

The mechanical properties of polydisperse polymer networks of mainly end-linked bimodal PDMS gels have been studied experimentally and been compared with theoretical predictions.[18] We have performed analogous uniaxial extension of our model systems and simulated the stress−strain response of polymer and polyelectrolyte networks. Starting with box lengths corresponding to equilibrium with pure water, the box lengths in the x, y, and z directions were scaled according to $L_x = L_0/\sqrt{\lambda}$, $L_y = L_0/\sqrt{\lambda}$, and $L_z = \lambda L_0$, where L_0 is the box length at equilbrium and λ the box extension ratio. Note that the volume of the system is conserved. The normal stress acting on the box was evaluated according to

$$\sigma_T = \sigma_{zz} - (\sigma_{xx} + \sigma_{yy})/2 \tag{8}$$

where σ_{xx}, σ_{yy}, and σ_{zz} are the diagonal components of the stress tensor. To avoid impulsive forces at hard-sphere contact, the hard-sphere potential in these simulations was replaced with the Lennard-Jones potential $U(r) = 4\epsilon[(\sigma/r)^{12} - (\sigma/r)^6]$ with the values $\epsilon = 1.0$ kJ/mol and $\sigma = 2.0$ Å truncated at $r = 2^{1/6}\sigma$ and shifted by ϵ, making the potential purely repulsive.

The simplest theoretical expression of the normal stress is based on the phantom Gaussian chains and is given by[4]

$$\sigma_T = \frac{N_{chain}}{V} k_B T(\lambda^2 - 1/\lambda) \tag{9}$$

where k_B is the Boltzmann factor and T the temperature. A more elaborated theory based on chains with Redner−des Cloizeaux statistics and the junction affine model gives[34]

$$\sigma_T = (\lambda N_{chain} k_B T/V)\left[\frac{\Theta}{2(\lambda^3 - 1)}\left(2\lambda^2 + \lambda^{-1} - \frac{3\lambda^2 \arctan(\sqrt{\lambda^3 - 1})}{\sqrt{\lambda^3 - 1}}\right) + \frac{\Theta + 3}{\lambda^{(t+5)/2}}\left(-{}_2F_1\left(\frac{1}{2}, \frac{1+t}{2}, \frac{3}{2}, 1 - \lambda^{-3}\right) + \frac{\lambda^{-3} + 2}{3}\,{}_2F_1\left(\frac{3}{2}, \frac{3+t}{2}, \frac{5}{2}, 1 - \lambda^{-3}\right)\right)\right] \tag{10}$$

where $\Theta = (\Gamma - 1)/\nu$ and $t = 1/(1 - \nu)$ are constants related to the critical exponents[35] Γ and ν of the polymer, and ${}_2F_1$ is the hypergeometric function defined by ${}_2F_1(a,b,c,z) = \sum_0^\infty[(a)^n(b)^n/(c)^n](z^n/n!)$ with $(x)^n = x(x+1)(x+2)...(x+n-1)$.

Figure 6a shows the normal stress for system 1 as a function of λ along with the two theoretical predictions. For the Gaussian theory ($N_{chain}/V)k_BT = 0.150$ MPa has been used and augmented with $\Gamma = 7/6$ and $\nu = 0.59$ for the non-Gaussian theory.[34] Generally, the simulated normal stress increases roughly exponentially with increasing box extension ratio. Such an upturn of the stress at high extensions has previously been observed by Mark and coauthors from experiments and simulations.[18,36] As the polydispersity index increases, the rise of the normal stress curve increases. At low extensions, the two theoretical approaches predict similar slopes (modulii), but in the case of eq 9, the result is a factor of 2 too low. At larger box extension ratios, the Gaussian theory (solid curve) strongly underestimates the normal stress, whereas the non-Gaussian theory (dashed curve) describes the increased normal stress at larger box extension ratios in a better manner.

The corresponding normal stress−strain relation for the polyelectrolye gel is displayed in Figure 6b. For the Gaussian theory $N_{chain}k_BT/V = 0.007\,53$ MPa, and for the non-Gaussian theory we have used values of $\Gamma = 1$ and $\nu = 0.88$. The simulated normal stress for the polyelectrolyte gel resembles that for the uncharged network. However, the normal stress is

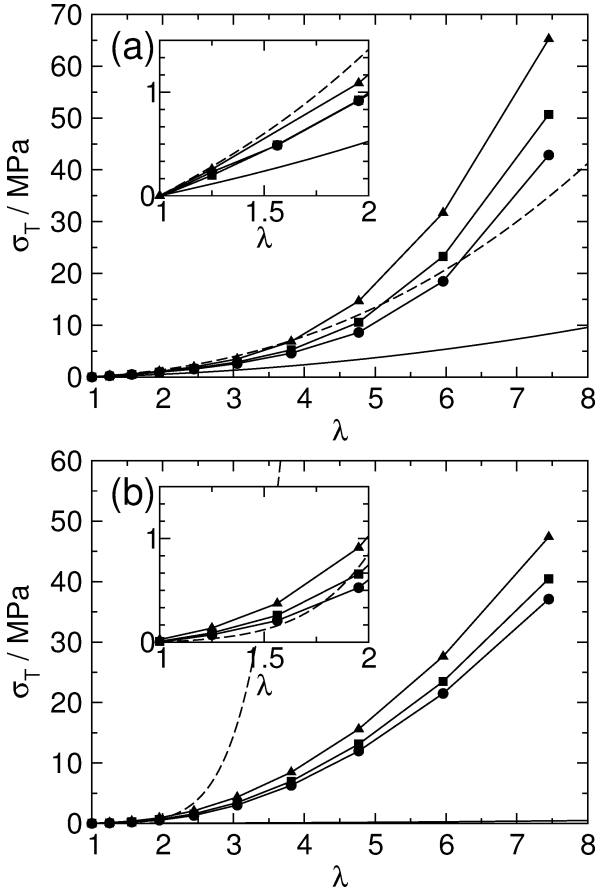

Figure 6. Normal stress σ_T as a function of the box extension parameter λ for (a) system 1 and (b) the reference system for $\gamma = 1$ (circles), $\gamma = 1.06$ (squares), and $\gamma = 1.16$ (triangles). Theoretical predictions based on eq 9 (solid curves) and on eq 10 (dashed curves) are also included. The values of the parameters for the theoretical predictions are given in the text. Errors are smaller than the symbol size.

smaller due to the fact that the chain density per unit area is smaller. Here, at small λ the Gaussian theory underestimates the normal stress by a factor 10. The non-Gaussian prediction is better than the Gaussian theory at small λ, but unlike for system 1, there is a crossover at $\lambda \approx 1.75$ whereafter the theory predicts a too large normal stress.

In summary, the volume of a polyelectrolyte gel is large and its network is under stress as shown by conformational as well as bond stretching analyses, owing to the osmotic pressure arising primarily from the confined counterions. A change from a monodisperse to a polydisperse chain length distribution with constant average chain length leads to (i) a reduced gel volume and (ii) the shorter chains becoming more stretched and under larger bond tension, whereas the longer chains become less stretched and under less tension, as compared to chains in the monodisperse network. The two observations are coupled. We attribute the reduced gel volume to the short chains which are highly extended, despite the presence of less-extended long chains. The uncharged polymer gel constitutes an exception; for this system the chain length polydispersity had only a marginal effect. The reason for the difference between charged and uncharged networks is that in the former case network chains are stronger stretched due to the osmotic pressure arising from the confined counterions, whereas in the latter case networks chains are only weakly stretched by the excluded-volume interaction. On studying the effect of different distributions of chains of different length in the network it was concluded that those with the shortest topological path responded

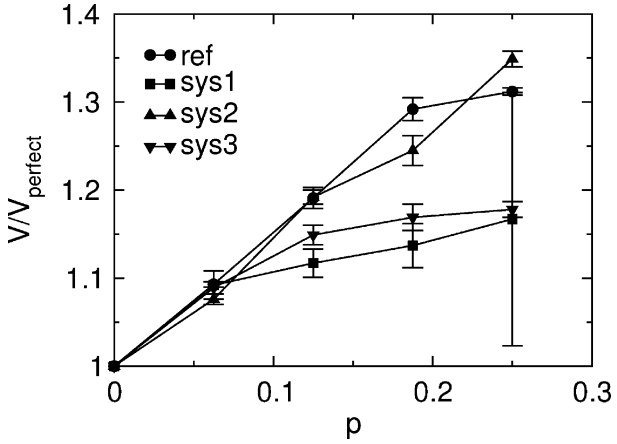

Figure 7. Volume ratio $V/V_{perfect}$ as a function of the fraction of inactive chains p for the reference system and systems 1−3. The large error in the last point for system 1 is due to the small slope of the pressure−volume isotherm at this inactive chain fraction.

strongest to a change in polydispersity. On increasing the fraction of short chains keeping the number of network beads constant, the volume decreases even further strengthening the view that it is the short chains that affect the volume in such networks. Upon uniaxial stretching, the simulated normal stress for both polyelectrolyte and polymer gels displayed roughly an exponential behavior with increasing λ. On comparison with the theory, the classical Gaussian theory gives lower stress in both cases studied but was better for the uncharged network. The non-Gaussian theory was comparably better than the Gaussian theory for both networks studied, but predicted a too large normal stress in the polyelectrolyte gel for $\lambda > 1.75$.

4.2. Topological Network Defects. The volume ratio $V/V_{perfect}$ as a function of the fraction of inactive chains p for the reference system and systems 1−3 is displayed in Figure 7. For all systems, we observe that the volume ratio increases continuously with increasing fraction of severed chains. As to the reference system, the volume increases by ≈35% at $p = 0.25$, i.e., 25% severed chains.

Regarding the uncharged system (system 1), the relative volume change upon breaking node−bead bonds is smaller. At $p = 0.25$ the volume has increased by 20%. The system with longer chains (system 2) displays a relative increase of its volume similar to that of the reference system upon introducing severed chains. The increase of the relative volume of the system with stiff chains (system 3) is smaller, in particular at the higher fraction of severed chains, as compared to that with flexible chains. Finally, the changes in volume on an absolute scale upon breaking node−bead bonds becomes different due to the different volumes of the perfect gels (given in Table 2). For example, the largest volume increase appears for system 3.

For polyelectrolyte gels with flexible chains (reference system and system 2), the increased gel volume on increasing number of inactive network chains is basically an effect of the reduced restoring force of the network counteracting the osmotic pressure contribution from the counterions. Even though the chains are severed at one end from a node, they are still attached to the network, and therefore their counterions remain in the network. The volume changes would have been different if those chains would have been detached at both ends and completely removed from the network. Regarding the uncharged system (system 1), the gel volume is essentially a balance between the excluded-volume interaction and the elastic contribution from the network. The smaller relative volume increase for the uncharged gel is a reflection of the smaller magnitude of these contributions.

Table 4. End-to-End Distance of Active and Severed Chains in Networks Containing Defects

system	p	$\langle R_{ee,a} \rangle$ (Å)	$\langle R_{ee,s} \rangle$ (Å)
	0	81.2	
ref	0.125	81.4	62.9
	0.25	84.4	64.5
	0	35.6	
sys1	0.125	35.3	33.4
	0.25	35.8	33.3
	0	167	
sys2	0.125	172	139
	0.25	182	141
	0	109	
sys3	0.125	111	107
	0.25	112	107

Finally, the smaller volume ratio increase of the gel with the stiff chains (system 3) is rationalized by a more rigid network.

We will now examine the stretching of the active and severed chains of the different systems. Table 4 provides the average end-to-end separations for the active $\langle R_{ee,a} \rangle$ and severed $\langle R_{ee,s} \rangle$ chains of some of the gels investigated. Throughout, (i) the severed chains are less stretched as compared to the active ones and (ii) the active ones become in some cases more stretched as the fraction of severed chains is increased. Again the behavior appears to be insensitive to the chain length of the polyelectrolyte gels (similar behavior for the reference system and system 2). The effect is smallest for the uncharged gel (system 1), rationalized by the fact that the active chains are only weakly stretched as discussed above. The variation of the chain extension of the stiff chains (system 3) is small due to the fact that the osmotic pressure of the counterions is small compared to the ref system and due to large bare persistence length of these chains.

Thus, the chains, which in the perfect gel are stretched due to the osmotic pressure from counterion entropy in polyelectrolyte gels and excluded-volume interactions in uncharged polymer gels, relax as the chains are severed. The relaxation is largest in the systems where the chains are strongest stretched by nonbonded interactions, i.e., polyelectrolyte gels with flexible chains.

5. Conclusions

Previous simulation studies of polyelectrolyte gels have been based on perfect polymer networks. In this contribution, we have examined (i) how volume and (ii) chain properties of polyelectrolyte gels and one uncharged gel in equilibrium with pure water are affected by chain length polydispersity and topological network defects. We have used a coarse-grained model where electrostatic interactions, excluded-volume effects, and network connectivity are the main components of the model. The properties of the model system were determined from Monte Carlo simulations with an isotropic variation of the box lengths.

As the network is made polydisperse, we found that the volume of polyelectrolyte gels decreases with the short chains being more stretched and the long ones less stretched as compared to a monodisperse chain length distribution. The relative volume decrease was largest for the polyelectrolyte networks and smallest for the uncharged gel. Upon uniaxial stretching, the simulated normal stress for polymer and polyelectrolyte gels displays roughly exponential behavior with increasing λ. On comparison with theories, a non-Gaussian theory was comparably better than the Gaussian theory for both gels studied, but still not quantitatively correct for large stretching.

Removing chain−node bonds leads to an increased gel volume and the severed chains become relaxed. The relative volume increase was most prominent for the polyelectrolyte gels with flexible chains and smaller for uncharged gels and polyelectrolyte gels with stiff chains. The large responses observed for the polyelectrolyte gels originates from the strong osmotic pressure contribution from the counterions appearing in the polyelectrolyte gel to electrostatically balance the network charge.

Our findings for the uncharged network agreed well with previous experimental and simulation studies. Since the primitive model has shown to accurately describe the electrostatic interaction in electrolyte and polyelectrolyte solutions, we are confident that the present simulation study is a first step of modeling polyelectrolyte gels with nonperfect network topologies.

Acknowledgment. Marcel van Eijk and Lennart Picullel are acknowledged for fruitful discussions at the initial part of this study. This work was partly financed by the Centre for Amphiphilic Polymers from Renewable Resources (CAP).

References and Notes

(1) Peppas, N. A.; Bures, P.; Leobandung, W.; Ichikawa, H. *Eur. J. Pharm. Biopharm.* **2000**, *50*, 27.
(2) Azzam, R. *Commun. Soil Sci. Plant Anal.* **1985**, *16*, 1123.
(3) Escobedo, F. A.; de Pablo, J. J. *Phys. Rep.* **1999**, *318*, 85.
(4) Everaers, R. *New J. Phys.* **1999**, *1*, 12.1.
(5) Schneider, S.; Linse, P. *Eur. Phys. J.* **2002**, *8*, 8030.
(6) Schneider, S.; Linse, P. *J. Phys. Chem. B* **2003**, *107*, 8030.
(7) Yan, Q.; de Pablo, J. J. *Phys. Rev. Lett.* **2003**, *91*, 018301.
(8) Lu, Z.-Y.; Hentschke, R. *Phys. Rev. E* **2003**, *67*, 061807.
(9) Schneider, S.; Linse, P. *Macromolecules* **2004**, *37*, 3850.
(10) Edgecombe, S.; Schneider, S.; Linse, P. *Macromolecules* **2004**, *37*, 10089.
(11) Mann, B. A.; Everaers, R.; Holm, C.; Kremer, K. *Europhys. Lett.* **2004**, *67*, 786.
(12) Mann, B. A.; Holm, C.; Kremer, K. *J. Chem. Phys.* **2005**, *122*, 154903.
(13) Edgecombe, S.; Linse, P. *Langmuir* **2006**, *22*, 3836.
(14) Andrady, A. L.; Llorente, M. A.; Mark, J. E. *J. Chem. Phys.* **1980**, *72*, 2282.
(15) Andrady, A. L.; Llorente, M. A.; Mark, J. E. *J. Chem. Phys.* **1980**, *73*, 1439.
(16) Llorente, M. A.; Andrady, A. L.; Mark, J. E. *Colloid Polym. Sci.* **1981**, *259*, 1056.
(17) Zhang, Z.-M.; Mark, J. E. *J. Polym. Sci., Polym. Phys. Ed.* **1984**, *20*, 473.
(18) Mark, J. E. *Acc. Chem. Res.* **1994**, *27*, 271.
(19) Hecht, A.-M.; Horkay, F.; Geissler, E. *J. Phys. Chem. B* **2001**, *105*, 5637.
(20) Kilian, H.-G. *Colloid Polym. Sci.* **1981**, *259*, 1151.
(21) Erman, B.; Mark, J. *Macromolecules* **1998**, *31*, 3099.
(22) Sommer, J.-U.; Lay, S. *Macromolecules* **2002**, *35*, 9832.
(23) Sommer, J.-U.; Saalwächter, K. *Eur. Phys. J. E* **2005**, *18*, 167.
(24) Michalke, W.; Lang, M.; Kreitmeier, S.; Göritz, D. *J. Chem. Phys.* **2002**, *117*, 6300.
(25) Pütz, M.; Kremer, K.; Everaers, R. *Phys. Rev. Lett.* **2000**, *84*, 298.
(26) Svaneborg, C.; Grest, G. S.; Everaers, R. *Polymer* **2005**, *46*, 4283.
(27) Doura, M.; Aota, H.; Masumoto, A. *J. Polym. Sci., Part A: Polym. Chem.* **2004**, *42*, 2192.
(28) Bastide, J.; Picot, C.; Candau, S. *J. Macromol. Sci., Phys.* **1981**, *B19*, 13.
(29) Patil, N. S.; Li, Y.; Rethwisch, D. G.; Dordick, J. S. *J. Polym. Sci., Part A: Polym. Chem.* **1997**, *35*, 2221.
(30) Allen, M. P.; Tildelsley, D. J. *Computer Simulation of Liquids*; Oxford University Press: New York, 1987.
(31) Friedberg, R.; Cameron, J. E. *Chem. J. Phys.* **1970**, *52*, 6049.
(32) Linse, P. MOLSIM 4.07 ed.; Lund University: Lund, 2004.
(33) Le Guilloi, J. C.; Zinn-Justin, J. *Phys. Rev. Lett.* **1977**, *39*, 95.
(34) Everaers, R. *Phys. J. II* **1995**, *5*, 1491.
(35) de Gennes, P.-G. *Scaling Concepts in Polymer Physics*; Cornell University Press: Ithaca, NY, 1979.
(36) Curro, J. G.; Mark, J. E. *J. Chem. Phys.* **1984**, *80*, 4521.
(37) Akinchina, A.; Linse, P. *Macromolecules* **2002**, *35*, 5183.

MA0700633